Inorg. Chem. **2006**, *45*, 5383–5392

Coordination Capabilities of a Novel Organic Polychlorotriphenylmethyl Monosulfonate Radical

Xavi Ribas,[†,‡] Daniel Maspoch,[†,#] Klaus Wurst,[§] Jaume Veciana,*[,†] and Concepció Rovira*[,†]

Departament de Nanociència Molecular i Materials Orgànics, Institut de Ciència de Materials de Barcelona, CSIC, Campus de la UAB, E-08193 Bellaterra, Spain, and Institut für Allgemeine Anorganische und Theoretische Chemie, Universitat Innsbruck, Innrain 52a, Innsbruck, Austria

Received February 1, 2006

The treatment of α-H-*p*-H-PTM (PTM = polychlorotriphenylmethane) with oleum 65% followed by deprotonation and oxidation leads to the isolation of a novel pure organic radical $PTMSO_3H\cdot 3H_2O\cdot 0.5$hexane (**2**). The X-ray diffraction of **2** reveals a layered structure with disordered H_2O molecules between facing sulfonic acid groups. We have explored the coordination abilities of the sulfonate derivative using different metals. The treatment of **2** with mild bases yields the sulfonate radical $PTMSO_3Na\cdot H_2O$ (**3**). On the other hand, the new compound $[Cu(py)_2(H_2O)_4](PTMSO_3)_2\cdot 2H_2O\cdot 2$EtOH (**4**) has been crystallized using Cu^{II} as the metallic counterion in the presence of pyridine. The structure reveals a solvent-separated ion-pair-type compound, with no direct coordination of the metal ion with the sulfonate group, and the formation of organic layers between layers of transition metal complexes. This situation has been overcome by favoring the stabilization of the sulfonate group over the Cu^{II} center by changing the pyridine ligand to cyclam. This has led to compound $[Cu(cyclam)](PTMSO_3)_2\cdot 6$EtOH (**5a**), in which the sulfonate group acts as a monodentate axial ligand for the Cu^{II} center. We have observed a single-to-single crystal rearrangement from **5a** to $[Cu(cyclam)](PTMSO_3)_2$ (**5b**) because of the loss of the solvent of crystallization, without significant modification of the metal coordination environment. All species have been structurally and magnetically characterized, and the magnetic coupling between the organic radicals and the metal paramagnetic centers is discussed.

Introduction

The search of materials exhibiting multiple functionalities has been the focus of intensive investigation in the molecular materials community. The combination of different physical properties in the same material and the observation of multistabilities simultaneously in different physical channels is a crucial step toward the design of new electronic, magnetic, or optical devices.[1] One of the extensively used approaches to synthesize functional materials is the metal−organic strategy for obtaining coordination polymers which incorporate open-shell transition metals. The precise control of the coordination geometry of the transition metal and the coordinating groups of the organic moieties account for the crystal engineering of the metal−organic polymers synthesized so far.[2] A step forward has been the incorporation of persistent stable organic radicals embedded in the coordination polymers in a manner such that the unpaired spins can magnetically interact.[3,4] Our group has recently reported several *para*- and *meta*-substituted polychlorotriphenylmethyl radicals (PTM)[5] with different numbers of carboxylic acid groups ($n = 1-6$)[6−8] that have been used as magnetically active building blocks for the synthesis of multifunctional materials. Exhaustive structural and magnetic studies have

* To whom correspondence should be addressed. E-mail: cun@icmab.es (C.R.); vecianaj@icmab.es (J.V.).
† Institut de Ciència de Materials de Barcelona.
§ Universitat Innsbruck.
‡ Current Address: Departament de Química, Universitat de Girona, Campus Montilivi, E-17071 Girona, Spain.
# Current Address: Institute for Nanotechnology, Northwestern University, 2145 Sheridan Road, Evanston, IL 60208.

(1) Itkis, M. E.; Chi, X.; Cordes, A. W.; Haddon, R. C. *Science* **2002**, *296*, 1443−1445.
(2) (a) Janiak, C. *Dalton Trans.* **2003**, *14*, 2781−2804. (b) Braga, D. *Chem. Commun*. **2003**, *22*, 2751−2754. (c) Eddaoudi, M.; Moler, D. B.; Li, H.; Chen, B.; Reineke, T. M.; O'Keeffe, M.; Yaghi, O. M. *Acc. Chem. Res.* **2001**, *34*, 319−330.
(3) (a) Caneschi, A.; Gatteschi, D.; Lalioti, N.; Sangregorio, C.; Sessoli, R.; Venturi, G.; Vindigni, A.; Rettori, A.; Pini, M. G.; Novak, M. A. *Angew. Chem., Int. Ed.* **2001**, *40*, 1760−1763. (b) Vaz, M. G. F.; Pinehiro, L. M. M.; Stumpf, H. O.; Alcantara, A. F. C.; Goleen, S.; Ouahab, L.; Cador, O.; Mathonière, C.; Kahn, O. *Chem.—Eur. J*. **1999**, *5*, 1486−1495. (c) Fegy, K.; Luneau, D.; Ohm, T.; Paulsen, C.; Rey, P. *Angew. Chem., Int. Ed. Engl*. **1998**, *37*, 1270−1273. (d) Culp, J. T.; Park, J.-H.; Meisel, M. W.; Talham, D. R. *Inorg. Chem*. **2003**, *42*, 2842−2848.

10.1021/ic060182j CCC: $33.50
Published on Web 06/15/2006

been performed on discrete copper(II) complexes bearing two axially coordinated PTMMC (monocarboxylated para-substituted PTM radical), showing three unpaired antiferromagnetically coupled ($2J/K_B = -30$ to -50 K) spins.[9] Furthermore, via the use of crystal engineering strategies on different PTM derivatives, a metal-organic nanoporous structure combining Cu^{II} ions and the PTMTC radical (tricarboxylated *para*-substituted PTM radical) was synthesized and described as a magnetic sponge with bulk magnetic ordering and with promising potential for application as a magnetic sensor.[10]

It is in this context that we decided to explore the substitution of the carboxylic functional group ($-$COOH) by a sulfonic group ($-SO_3H$) in the PTM radicals to investigate its potential use as a magnetically active building block for metal−organic coordination compounds. Herein, we report the synthesis of the PTM$-SO_3H$ radical and the coordinative possibilities of the deprotonated sulfonic group in its use as a magnetically active organic ligand. Although the sulfonate anion is generally considered to be a poor ligand,[11] with many examples of weakly interacting or noninteracting sulfonates found in the literature,[12] there is an increasing interest in the exploration of the sulfonate group as an efficient ligand for metals to form metal−organic layered structures,[13] as an analogy to the metal−phosphonate structures.[14] In general, the sulfonate group cannot displace H_2O molecules from the primary coordination sphere of the metal. However, alkali ions, large alkaline earth ions, and Ag(I) ions have been shown to be exceptions to the general trend.[13] The difference seems to rely on the nonpreferences for a coordination number or geometry. Indeed, the cooperative interactions in the formation of extended structures such as $AgPhSO_3$, AgOTs, and Ag(4-pyridinesulfonate) were reported to be responsible for the robustness of these structures, with thermal stabilities higher than 300 °C.[15] The cooperative interactions have been attributed to the spherical trioxy anionic sulfonate groups because they allow multiple connectivities to the metal centers.[16] With these bibliographic precedents, we have explored, for the first time, the coordination capabilities of a stable organic radical bearing a sulfonate group, and two examples with a nonparamagnetic alkaline metal ion and a paramagnetic transition metal ion such as Cu^{II} are presented. In the latter compound, we will demonstrate that a solvent-separated ion pair (SSIP) situation in the structure precludes magnetic communication between the two distinct magnetic centers. We will also show that it is possible to force direct coordination of the sulfonate group to the copper center and discuss the magnetic consequences.

Experimental Section

Materials. Solvents of reagent grade quality supplied by SDS were dried before use with a standard method and stored under Ar. Reagents were obtained commercially from Aldrich and used without further purification.

Elemental analyses were performed by SA−UAB (Servei d'Anàlisi−Universitat Autònoma de Barcelona). UV−vis−NIR spectra were recorded on a Varian Cary 5 spectrophotometer. IR spectra were obtained on a Perkin-Elmer Spectrum One spectrophotometer using KBr pellets. Cyclic voltammetry experiments were carried out at room temperature with an EG&G (PAR263A) potentiostat-galvanostat in a normal three-electrode cell (Ag/Ag^+ reference) with Pt wires as working and auxiliary electrodes. Distilled and argon-degassed methanol or acetonitrile were used as solvents with 0.1 M $(n\text{Bu}_4\text{N})^+PF_6^-$ as supporting electrolyte (scan rate = 100 mV s^{-1}). Thermogravimetric analyses were performed under argon with a high sensitivity Perkin-Elmer TGA7 balance.

X-ray powder diffraction studies were performed in the Serveis Científico-Tècnics de la UB. The polycrystalline samples were gently ground and placed in Lindemann capillary tubes of 0.2 mm of diameter. A Debye−Scherrer geometry diffractometer INEL CPS-120 (radius = 250 mm) was used. The radiation used was Cu Kα1 (λ = 1.540598 Å), with a working power of 40 KV (30 mA). The detector was sensitive to 120° position, with 4096 measure channels. The equipment contents a Germanium(111) flat primary monochromator and a reflector mirror from OSMIC Gutman Optics (13B-413). The beam height was 2−3 mm for all samples, and its width was 0.1 mm. Calibration was performed using $Na_2Ca_2Al_2F_{13}$ (NAC) as an external reference (cubic function SPLINE). Linearization was done with the PEAKOC software (from INEL). Typical measurement times were about 3 h.

(4) (a) Minguet, M.; Luneau, D.; Lhotel, E.; Vincent Villar, Paulsen, C.; Amabilino, D. B.; Veciana, J. *Angew. Chem., Int. Ed*. **2002**, *41*, 586−589. (b) Vostrikova, K. E.; Luneau, D.; Wernsdorfer, W.; Rey, P.; Verdaguer, M. *J. Am. Chem. Soc*. **2000**, *122*, 718−719. (c) Oshio, H.; Ito, T. *Coord. Chem. Rev*. **2000**, *198*, 329−346. (d) Marvilliers, A.; Pei, Y.; Cano, J.; Vostrikova, K. E.; Paulsen, C.; Rivière, E.; Audière, J.-P.; Mallah, T. *Chem. Commun*. **1999**, 1951−1952. (e) Field, L. M.; Lahti, P. M.; Palacio, F. *Chem. Commun*. **2002**, 636−637. (f) Stroh, G.; Turek, P.; Rabu, P.; Ziessel, R. *Inorg. Chem*. **2001**, *21*, 5334−5342. (g) Min, K. S.; Rhinegold, A. L.; Miller, J. S. *Inorg. Chem*. **2005**, *44*, 8433−8441.

(5) Ballester, M. *Acc. Chem. Res*. **1985**, *12*, 380−387.

(6) (a) Maspoch, D.; Gerbier, P.; Catala, L.; Vidal-Gancedo, J.; Wurst, K.; Rovira, C.; Veciana, J. *Chem.−Eur. J*. **2002**, *8*, 3635−3645. (b) Roques, N.; Maspoch, D.; Domingo, N.; Ruiz-Molina, D.; Wurst, K.; Tejada, J.; Rovira, C.; Veciana, J. *Chem. Commun*. **2005**, 4801−4803. (c) Maspoch, D.; Domingo, N.; Ruiz-Molina, D.; Wurst, K.; Tejada, J.; Rovira, C.; Veciana, J. *C. R. Chem.* **2005**, *8*, 1213.

(7) Maspoch, D.; Domingo, N.; Ruiz-Molina, D.; Wurst, K.; Tejada, J.; Rovira, C.; Veciana, J. *J. Am. Chem. Soc*. **2004**, *126*, 730−731.

(8) Maspoch, D.; Domingo, N.; Ruiz-Molina, D.; Vaughan, G.; Wurst, K.; Tejada, J.; Rovira, C.; Veciana, J. *Angew. Chem., Int. Ed.* **2004**, *43*, 1828−1832.

(9) (a) Maspoch, D.; Ruiz-Molina, D.; Wurst, K.; Rovira, C.; Veciana, J. *Dalton Trans.* **2004**, 1073−1082. (b) Maspoch, D.; Ruiz-Molina, D.; Wurst, K.; Rovira, C.; Veciana, J. *Chem. Commun.* **2004**, 1164−1165. (c) Maspoch, D.; Ruiz-Molina, D.; Wurst, K.; Rovira, C.; Veciana, J. *Chem. Commun.* **2002**, 2958−2959.

(10) Maspoch, D.; Ruiz-Molina, D.; Wurst, K.; Domingo, N.; Cavallini, M.; Biscarini, F.; Tejada, J.; Rovira, C.; Veciana, J. *Nature Mater*. **2003**, *2*, 190−195.

(11) Davies, J. A.; Hockensmith, C. A.; Kukushkin, V. Y.; Kukushkin, Y. N. *Synthetic Coordination Chemistry: Principles and Practice*; World Scientific: London, 1996; p 58.

(12) (a) Lawrence, G. A. *Chem. Rev.* **1986**, *86*, 17−33. (b) Smith, G.; Cloutt, B. A.; Lynch, D. E.; Byriel, K. A.; Kennard, C. H. L. *Inorg. Chem*. **1998**, *37*, 3236−3242. (c) Dalrymple, A. A.; Shimizu, G. K. H. *Chem. Commun*. **2002**, 2224−2225.

(13) Coté, A. P.; Shimizu, G. K. H. *Coord. Chem Rev*. **2003**, *245*, 49−64.

(14) (a) Kaschak, D. M.; Johnson, S. A.; Hooks, D. E.; Kim, H.-N.; Ward, M. D.; Mallouk, T. E. *J. Am. Chem. Soc.* **1998**, *120*, 10887−10894. (b) Clearfield, A. *Prog. Inorg. Chem*. **1998**, *47*, 371−510.

(15) (a) Shimizu, G. K. H.; Enright, G. D.; Ratcliffe, C. I.; Rego, G. S.; Reid, J. L.; Ripmeester, J. A. *Chem. Mater*. **1998**, *10*, 3282−3283. (b) Shimizu, G. K. H.; Enright, G. D.; Ratcliffe, C. I.; Preston, K. F.; Reid, J. L.; Ripmeester, J. A. *Chem. Commun*. **1999**, 1485−1486. (c) May, L. J.; Shimizu, G. K. H. *Chem. Mater*. **2005**, *17*, 217−220.

(16) Mäkinen, S. K.; Melcer, N. J.; Parvez, M.; Shimizu, G. K. H. *Chem.−Eur. J.* **2001**, *7*, 5176−5182.

The synthesis of the α-H-*p*-H-PTM precursor was performed according to the procedure described in the literature.[17]

α-H-PTMSO$_3$H (1). A solution of 1.8 g (2.48 mmol) of α-H-*p*-H-PTM in 40 mL of 65% oleum was heated at 95 °C with stirring for 60 h. The reaction mixture was cooled to room temperature and poured over ice (150 mL). The solid precipitate was filtered, rinsed with H_2O, and dissolved in 100 mL of $CHCl_3$. The addition of a saturated solution of $NaHCO_3$ (100 mL) allowed the sulfonate sodium salt to dissolve in the aqueous fraction. The latter was acidified with concentrated aqueous HCl until a permanent acid pH and extracted with $CHCl_3$ (3 × 200 mL). The latter solution was dried with anhydrous Na_2SO_4, filtered, and evaporated. The solid was purified by column chromatography (silica gel/acetone). The product was decolored by dissolving it in 50 mL of $CHCl_3$ and left over active carbon for 3 days, followed by a second purification by column chromatography. The aliquots of the product were evaporated giving 1.05 g (1.30 mmol) of α-H-PTMSO$_3$H (**1**). MW: 806.62 g/mol. Yield: 53%.

PTMSO$_3$H·3H$_2$O·0.5hexane (2). To a solution of 100 mg (0.124 mmol) of α-H-PTMSO$_3$H (**1**) in 10 mL of freshly distilled DMSO, 0.5 g (0.0125 mol) of smashed NaOH was added. The suspension was placed in an automatic shaker during 24 h in a dark room. The intense red solution was then filtered, and 37 mg (0.146 mmol) of resublimated I_2 were added; the mixture was shaken and left for 1 h. Twenty milliliters of a solution of aqueous $NaHSO_3$ (3.9%) were added, followed by acidification with concentrated HCl until a permanent acidic pH. The compound was extracted with $CHCl_3$, dried with anhydrous Na_2SO_4, and evaporated. The dark-red powder was chromatographied in column with silica gel and eluted with acetone. The product was redissolved in $CHCl_3$ and recolumnated in the same conditions yielding 85 mg (0.011 mmol) of a dark-red powder corresponding to **2**. MW: 805.62 g/mol. Yield: 85%. Compound **2** was recrystallized from $CHCl_3$/*n*-hexane producing block-shaped crystals of PTMSO$_3$H·3H$_2$O·0.5hexane (**2**).

UV−vis (THF): λ_{max} (ϵ) 285 (6500), 368 (16 800), 385 (32 600), 505 (1000), 565 nm (920 cm^{-1} M^{-1}). IR (KBr pellet): ν 2928, 2223, 1508, 1337, 1307, 1258, 1200, 1132, 1117, 1060, 818, 739, 713,695, 671, 659, 602, 515 cm^{-1}. Anal. Calcd (%) for $C_{19}Cl_{14}SO_3H·2H_2O$: C, 27.11; S, 3.80; H, 0.60; Cl, 58.98. Found: C, 26.91; S, 3.74; H, 0.56; Cl, 59.30. CV (in CH_2Cl_2): $E_{1/2}$ (vs Ag/AgCl) −0.13 V. EPR (CH_3CN/toluene 1/1): $g = 2.0023$ (ΔH_{pp} = 4.0 G), no half-field signal.

PTMSO$_3$Na·H$_2$O (3). Fifty milligrams (0.0621 mmol) of the PTMSO$_3$H radical (**2**) was dissolved in 20 mL of THF, and an excess $NaHCO_3$ (20 mL of a saturated solution) was added to produce a precipitate that was filtered and dried under vacuum. The solid obtained was recrystallized from a mixture of THF and hexane yielding 45 mg (0.053 mmol) of red plate-shaped crystals of the PTMSO$_3$Na·H$_2$O radical salt (**3**). MW: 845.61 g/mol. Yield: 86%. UV−vis (THF): λ_{max} (ϵ) 269 (sh, 13 800), 386 (27 200), 425 (sh, 2500), 510 (sh, 860), 566 nm (800 cm^{-1} M^{-1}). IR (KBr pellet): ν 2926, 2856, 1510,1337, 1307, 1255, 1224, 1117, 1065, 818, 713, 671, 603, 515 cm^{-1}. Anal. Calcd (%) for $C_{19}Cl_{14}SO_3Na·1H_2O$: C, 26.99; S, 3.79; H, 0.24. Found: C, 27.36; S, 3.90; H, 0.48. CV (in CH_2Cl_2/THF 99/1): $E_{1/2}$ (vs Ag/AgCl) −0.16 V. EPR (CH_3CN/toluene 1/1): $g = 2.0020$ (ΔH_{pp} = 1.0 G), no half-field signal. EPR (on oriented single crystal): $g_{min} = 2.0014$ (ΔH_{pp} = 8.9 G), $g_{max} = 2.0022$ (ΔH_{pp} = 2.86 G).

[Cu(py)$_2$(H$_2$O)$_4$](PTMSO$_3$)$_2$·2H$_2$O·2EtOH (4). Twenty-five milligrams (0.031 mmol) of PTMSO$_3$H radical (**2**) dissolved in 1 mL of ethanol was added dropwise to a solution of 3.8 mg (0.016 mmol) of Cu(NO$_3$)$_2$·3H$_2$O in a mixture of 5 mL of ethanol, 0.5 mL of H_2O, and 3 drops of pyridine (large excess). Immediately after the addition, the solution was filtered and left to stand at room temperature for several days, until the appearance of 24 mg (0.012 mmol) of red-block crystals corresponding to compound **4**. MW: 1995.17 g/mol. Yield: 78%. IR (KBr pellet): ν 3435, 1656, 1609, 1449, 1336, 1305, 1256, 1212, 1115, 1060, 1017, 874, 817, 697, 669, 602, 515 cm^{-1}. Anal. Calcd (%) for $C_{52}Cl_{28}S_2N_2H_{34}O_{14}Cu$: C, 30.75; S, 3.16; H, 1.69; N, 1.38. Found: C, 30.50; S, 3.10; H, 1.75; N, 1.45. EPR (on solid, 298 K): $g_1 = 2.0060$ (ΔH_{pp} = 35 G), $g_2 = 2.265$. EPR (on solid, 120 K): $g_1 = 2.0097$ (ΔH_{pp} = 42 G), $g_2 = 2.2418$.

[Cu(cyclam)](PTMSO$_3$)$_2$·6EtOH (5a) and [Cu(cyclam)](PTMSO$_3$)$_2$ (5b). Fifty-two milligrams (0.063 mmol) of PTMSO$_3$Na radical (**3**) dissolved in 20 mL of ethanol was placed at the bottom of a glass tube. A solution of 7.6 mg (0.031 mmol) of Cu(NO$_3$)$_2$·6H$_2$O and 6.3 mg of cyclam (1,4,8,11-tetraazacyclotetradecane) in 20 mL of ethanol was then carefully added. The self-diffusion of both solutions resulted in the precipitation of 20 mg (0.011 mmol) of red crystals after 4 days, corresponding to compound **5a.** The crystals lost all the solvent of crystallization after removal from the mother liquor, suffering a crystal-to-crystal reorganization resulting in compound **5b** (see text). MW (**5b**): 1873.11 g/mol. Yield (**5b**): 35%. IR (KBr pellet): ν 3436, 3196, 2923, 2849, 1631, 1458, 1429, 1137, 1306, 1213, 1114, 1058, 817, 670, 601, 514 cm^{-1}. Anal Calcd (%) for $C_{48}Cl_{28}S_2N_4H_{24}O_6Cu$: C, 30.78; S, 3.52; H, 1.29; N, 2.99. Found: C, 30.64; S, 3.65; H, 1.10; N, 2.86. EPR (on solid, 298 K): $g_1 = 2.0199$ (ΔH_{pp} = 11.4 G), $g_2 = 2.0670$. EPR (on solid, 120 K): $g_1 = 2.0206$ (ΔH_{pp} = 12.9 G), $g_2 = 2.0681$.

Compound **5a** has been characterized by X-ray diffraction studies on one crystal in mother liquor.

Crystallographic Determination. Crystals for X-ray determination (see Supporting Information) were grown by hexane diffusion into a $CHCl_3$ solution of compound **2** and from direct synthesis in ethanol for compounds **4** and **5a**. The structure of compound **5b** was obtained from the measurement of the **5a** crystal mounted in a capillary after evaporation of the ethanol molecules of crystallization. Crystal data was collected on a Nonius Kappa CCD diffractometer with graphite-monochromated Mo Kα radiation (λ = 0.71073 Å) at 233(3) K for **2** and **4** and 290(2) K for **5a**/**5b**. Intensities were integrated using DENZO and scaled with SCALEPACK. Several scans in the ϕ and ω directions were made to increase the number of redundant reflections, which were averaged in the refinement cycles. This procedure replaces an empirical absorption correction. The structure was solved with direct methods (SHELXS86) and refined against F^2 (SHELX97).[18] Hydrogen atoms at the carbon atoms were added geometrically and refined using a riding model. Hydrogen atoms at the disordered solvent H_2O and hexane molecules were omitted for **2** and found and refined with bond restraints for the H_2O and ethanol molecules of **4**. All non-hydrogen atoms were refined with anisotropic displacement parameters.

The quality of the crystals will be reflected by their diffraction power and mosaicities, whereas small crystals, disordered parts in the unit cell, and high crystal mosaicities often reduce the diffraction power. For a good measurement with our Nonius KappaCCD, we need crystals with a mosaicity of 0.4−0.6 and a size of around 0.2 × 0.2 × 0.2 mm^3, whereas the size depends more precisely on the number the heavy atoms and the size of the unit cell. These criteria

(17) Ballester, M.; Riera, J.; Castanyer, J.; Rovira, C.; Armet, O. *Synthesis* **1986**, 64−66.

(18) Sheldrick, G. M. *SHELXL97: Program for the Refinement of Crystal Structures*; University of Göttingen: Göttingen, Germany, 1997.

Table 1. Crystal Data and Structure Refinement of Compounds **2**, **4**, **5a**, and **5b**

	2	**4**	**5a**	**5b**
formula	$C_{22}H_{14}Cl_{14}O_6S$	$C_{52}H_{34}Cl_{28}CuN_2O_{14}S_2$	$C_{60}H_{60}Cl_{28}CuN_4O_{12}S_2$	$C_{48}H_{24}Cl_{28}CuN_4O_6S_2$
fw	902.69	2031.07	2149.38	1872.97
cryst system	monoclinic	triclinic	triclinic	triclinic
space group	$P2_1/c$	$P\bar{1}$	$P\bar{1}$	$P\bar{1}$
a (Å)	25.3000(10)	8.7847(3)	8.760(3)	8.730(2)
b (Å)	15.3074(6)	8.8026(2)	15.449(6)	8.775(2)
c (Å)	18.6765(7)	24.6455(8)	16.617(5)	22.060(6)
α (deg)	90	84.876(2)	84.77(2)	95.95(2)
β (deg)	99.957(2)	87.119(2)	83.07(2)	94.83(2)
γ (deg)	90	82.879(2)	82.44(1)	95.92(2)
V (Å$^{3)}$	7124.0(5)	1882.05(10)	2206.5(13)	1664.1(7)
Z	8	1	1	1
D_c (g cm^{-3})	1.683	1.792	1.618	1.869
T)K)	233(2)	233(2)	290(2)	290(2)
λ(Mo Kα) (Å)	0.71073	0.71073	0.71073	0.71073
μ (mm^{-1})	1.177	1.400	1.198	1.566
2θ max (deg)	21.00	24.99	17.50	17.50
reflns collected	25 957	7381	4691	3435
independent reflns	7582 (R_{int} = 0.0772)	5456 (R_{int} = 0.0233)	2683 (R_{int} = 0.0984)	2048 R_{int} = 0.0600
params	743	477	348	283
GOF on F^2	1.033	1.079	1.055	1.114
R/R_w[a]	0.0687/0.1670	0.0400/0.0882	0.0932/0.1761	0.0986/0.1885

[a] $R = \sum|F_o - F_c|/\sum F_o$ and $R_w = \{\sum[w(F_o^2 - F_c^2)^2]/\sum[w(F_o^2)^2]\}^{1/2}$ where $w = 1/[\sigma^2(F_o^2 + (aP)^2 + bP]$, $P = (F_o^2 + 2F_c^2)/3$, and the a and b are constants given in the Supporting Information.

Scheme 1

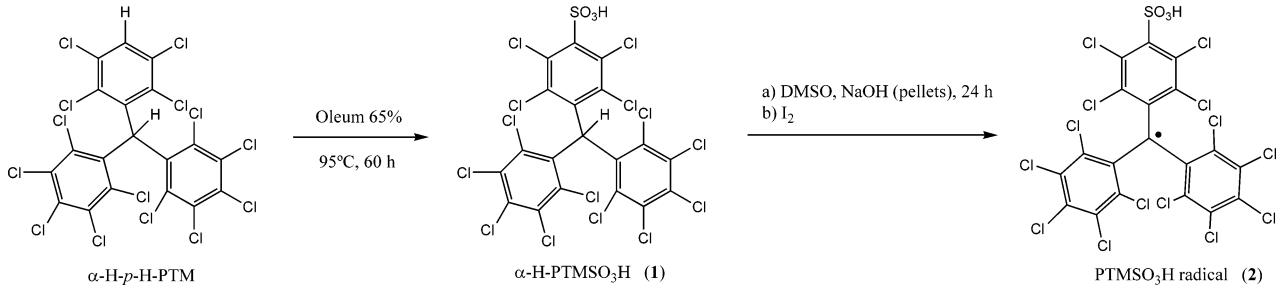

are fulfilled only for **4** with size of 0.4 × 0.2 × 0.1 mm^3 and a mosaicity of 0.6. The diffraction power of **2**, with size of 0.4 × 0.2 × 0.02 mm^3 and mosaicity of 0.8, is more reduced by the crystal size, and visible reflections on the frames could be seen only to a 2Φ value of 38°. The measurements of **5a** and **5b** were difficult because the crystals immediately lose solvent ethanol, and therefore, the **5a** crystals were placed in a glass-capillary with mother liqueur. The crystal size of **5a** was only 0.2 × 0.07 × 0.03 mm^3 and the mosaicty of 1.9 is extremely high, therefore reflections on the frames were seen only to a 2Φ value of 28°. Because of the fewer reflections, carbon atoms could only be refined with isotropic displacement parameters. After two weeks, the mother liqueur was reduced by about the half because of a leak in the capillary, and the same crystal was remeasured with a mosacity of 2.5 and the lattice constants of **5b**.

Further details of the crystal structure determinations are given in Table 1. Graphical representations were prepared using the Mercury 1.4 (CCDC) program.

Magnetic Measurements. EPR spectra of **2**−**4** and **5b** were obtained in a conventional X-band spectrometer (Bruker ESP 300 E) equipped with a microwave bridge ER041XK, a rectangular cavity operating in T102 mode, a field controller ER 032M system, and a Oxford ESR-900 cryostat, which enabled measurements in the temperature range of 110−350K. The temperature was monitored by a Au (0.07 at % Fe)−chromel thermocouple placed close to the sample. The measurements were performed on a bulk polycrystalline sample, placed inside a quartz tube, and in solution. The modulation amplitude was kept well below the line width and the microwave power well below saturation.

The static magnetic susceptibilities of polycrystalline randomly oriented samples of **2**, **3**, **4** and **5b** were measured in the temperature range of 2−300 K with a Quantum Design MPMSXL superconducting SQUID magnetometer operating at a magnetic field strength of 0.5 T. The paramagnetic susceptibility was calculated with a diamagnetic correction estimated from tabulated Pascal constants.

Results and Discussion

Synthesis of PTMSO$_3$H·3H$_2$O·0.5hexane (2). Radical PTMSO$_3$H was synthesized by a two-step procedure starting from *p*-H-polychlorotriphenylmethane (α-H-*p*-H-PTM),[17] as shown in Scheme 1. The introduction of the sulfonic group at the para position of one of the phenyl rings bearing the *p*-H atom was achieved by dissolving α-H-*p*-H-PTM in 65% oleum and heating the mixture at 90 °C for 90 h. Successive acid and basic extractions afforded compound α-H-PTMSO$_3$H (**1**) in moderate yield. The PTMSO$_3$H radical was formed by oxidation of the corresponding anion previously obtained by deprotonation of the α-H precursor (Scheme 1). The target compound PTMSO$_3$H radical was isolated as a crystalline material in good yield. Recrystallization of the red crystalline material in CHCl$_3$/*n*-hexane yielded red block-shaped crystals suitable for single-crystal X-ray diffraction. The compound

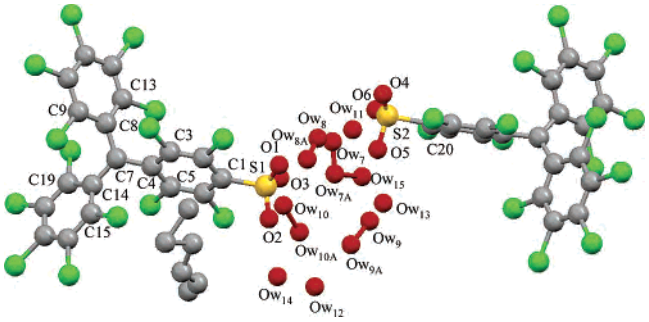

Figure 1. Asymmetric unit of the radical $PTMSO_3H{\cdot}3H_2O{\cdot}0.5$hexane (**2**) structure (representative atoms labeled).

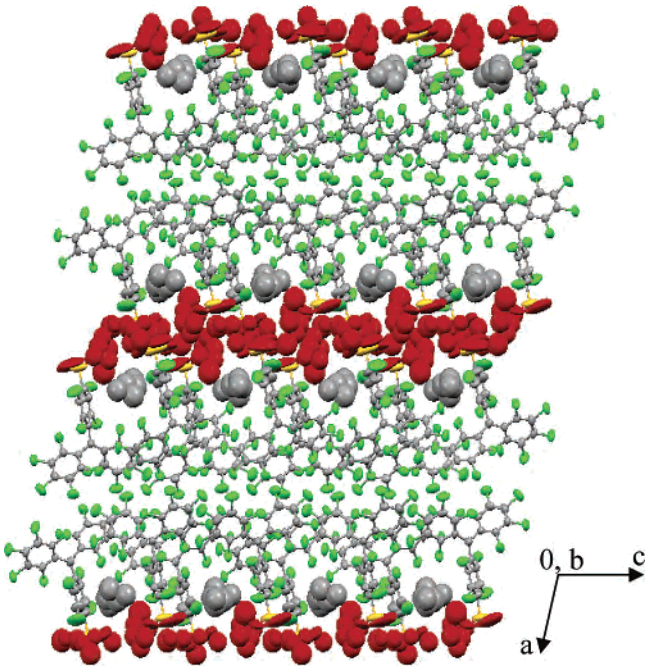

Figure 2. Ellipsoid (50%) mode representation of the crystal packing of $PTMSO_3H{\cdot}3H_2O{\cdot}0.5$hexane (**2**).

with formula $PTMSO_3H{\cdot}3H_2O{\cdot}0.5$hexane (**2**) crystallizes in the monoclinic system, space group $P2_1/c$ (Table 1 and Table S1, see Supporting Information). The asymmetric unit contains two different $PTMSO_3H$ radicals, six H_2O molecules disordered in different positions with occupancies from 0.67 to 0.33, and one *n*-hexane molecule with high mobility (Figure 1). The sulfonic oxygen atoms present a high connectivity with the O atoms of the H_2O molecules, but the disorder in the water positions precludes a detailed description. The crystal packing of **2** shows an alternated layered polar−apolar structure along the *a* direction, with a 2D network of water−sulfonic interactions as the polar layer and a 2D layer formed by the organic chlorinated part of the $PTMSO_3H$ molecules as the apolar counterpart, with one molecule of *n*-hexane embedded in the interface of both layers (Figure 2). The apolar layer is stabilized by multiple Cl···Cl contacts,[19] a supramolecular motif commonly observed in PTM-type compounds.

(19) For a study of Cl···Cl contacts, see: (a) Sarma, J. A. R. P.; Desiraju, G. R. *Acc. Chem. Res.* **1986**, *19*, 222. (b) Desiraju, G. R.; Parthasarathy, R. *J. Am. Chem. Soc.* **1989**, *111*, 8725−8726.

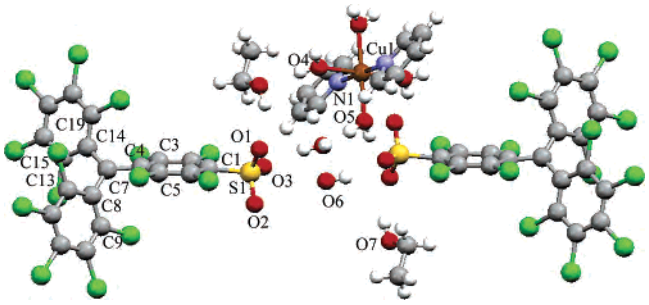

Figure 3. Structure of $[Cu(py)_2(H_2O)_4](PTMSO_3)_2{\cdot}2H_2O{\cdot}2$EtOH (**4**) (representative atoms labeled).

$PTMSO_3Na{\cdot}H_2O$ (3). The synthesis of this alkaline salt was easily achieved by the deprotonation of the $PTMSO_3H$ radical (**2**) with a mild base ($NaHCO_3$). The recrystallization of the resulting red powder in THF/hexane produced red plate-shaped crystals that could not be properly resolved by X-ray diffraction because of the low quality of crystals.[20] This low-quality structural determination precludes the correct assignment of the electron densities found between the sulfonate groups: it is probably a mixture of Na ions and H_2O molecules.

$[Cu(py)_2(H_2O)_4](PTMSO_3)_2{\cdot}2H_2O{\cdot}2$EtOH (4). The synthesis of this compound was achieved by the diffusion of a solution of an excess of pyridine in ethanol to an ethanolic solution of the $PTMSO_3H$ radical (**2**) and $Cu^{II}(NO_3)_2{\cdot}6H_2O$. The pyridine acted at the same time as a base to deprotonate the sulfonic acid to the sulfonate group and as a ligand for the Cu^{II} dication. This strategy resembled the one used for the synthesis of a metal−organic porous compound named MOROF-1.[10] The choice of nitrate as a counteranion for the copper source was made because of its low coordinative abilities to exclude it as a competitor of the sulfonate group in the possible formation of the complex.

Compound **4** crystallizes as red prismatic crystals in the triclinic system, space group $P\bar{1}$ (Table 1). The asymmetric unit contains one copper atom located on a symmetric center and one molecule of $PTMSO_3^-$, one coordinated pyridine, two coordinated H_2O molecules, and one H_2O and EtOH molecules of crystallization in general positions (Figure 3). The structure of **4**, with a stoichiometry of two $PTMSO_3^-$ molecules per copper ion, reveals that there is no direct coordination of the sulfonate group with the Cu^{II} cation; thus it acts as a counteranion of the Cu^{II} dication. Indeed, the metal ion shows a hexacoordination to two pyridine and two H_2O molecules in the equatorial plane and to two additional H_2O molecules in the axial positions. In contrast with the structure of **3**, no disorder is found on the O atoms of the sulfonate groups. This allows one to clearly determine the strong H-bonding network between the sulfonate groups, H_2O, and ethanol molecules of the structure. The three O atoms of each sulfonate group show two H-bonds with the

(20) The diffraction image of **3** was similar to **2**, in the sense that almost the same crystal cell was obtained showing an alternated layered polar−apolar structure as in **2**. But in this case, the quality reduction comes more from the mosaicity of 1.4 than from the size of 0.45 × 0.35 × 0.1 mm^3. Three further crystals of **3** were examined, but all had higher mosaicities.

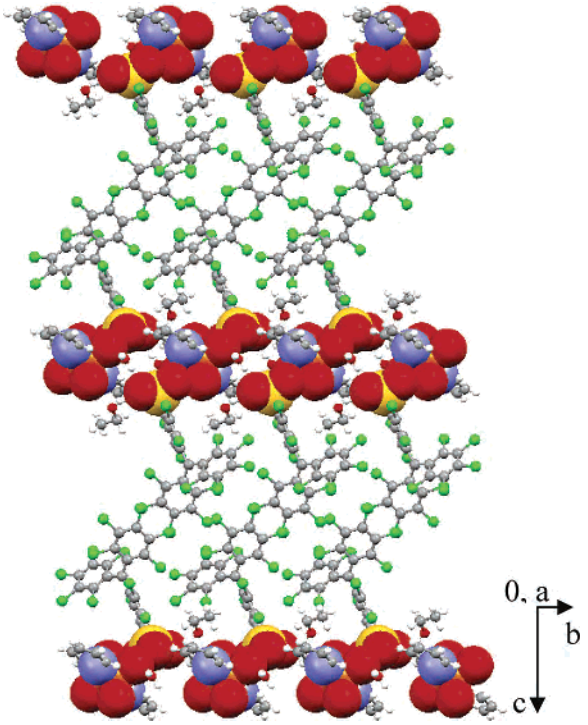

Figure 4. Crystal packing of $[Cu(py)_2(H_2O)_4](PTMSO_3)_2 \cdot 2H_2O \cdot 2EtOH$ (**4**) (copper coordination environment and sulfonate groups depicted in the space-filling mode).

H_2O molecules directly coordinated to a copper center, two other H-bonds with H_2O molecules of crystallization, and one additional H-bond with an ethanol molecule of crystallization (Table S1, see Supporting Information). An additional H-bond exists between each ethanol molecule and one H_2O molecule axially coordinated to the copper atom, and there is also another H-bond between each H_2O molecule of crystallization and one of the equatorially coordinated H_2O molecules. Overall, this leads to a complex supramolecular organization in which each $PTMSO_3^-$ unit participates in the formation of one $R^6_6(16)$, one $R^3_4(10)$, and one $R^2_2(8)$ cyclic hydrogen-bonded motifs (Figure S1, see Supporting Information). Simultaneously, each Cu^{II} complex contributes to the formation of two of each one. Additionally, a torsion of 55.4° is observed for the pyridine planes with respect to the equatorial plane around the copper center that may be related to the supramolecular $\pi\cdots$H−C interaction with the methyl group of the ethanol molecule of crystallization (pyridine centroid···H26B−C26 distance of 3.106 Å).

The crystal packing of **4** reveals the formation of alternating organic/inorganic 2D layers (Figure 4). Each organic layer is built up by the interaction of the chlorinated organic part of the $PTMSO_3^-$ molecules in the *c* direction, whereas the inorganic layer is formed by Cu complex molecules along the *c* axis. Thus, the layers are connected by an intricate network of strong H-bonds but with no direct coordination of the charge-carrier atoms (i.e., the sulfonate group and the copper center). The latter allows defining this structure as an example of a solvent-separated ion pair (SSIP).

[Cu(cyclam)](PTMSO$_3$)$_2$·6EtOH (5a). The synthesis of this compound was achieved by diffusing a previously prepared ethanolic solution of $Cu^{II}(NO_3)_2 \cdot 6H_2O$ and the cyclam ligand (to form the cationic complex $[Cu(cyclam)]^{2+}$) into an ethanolic solution of the $PTMSO_3Na$ radical (**3**).

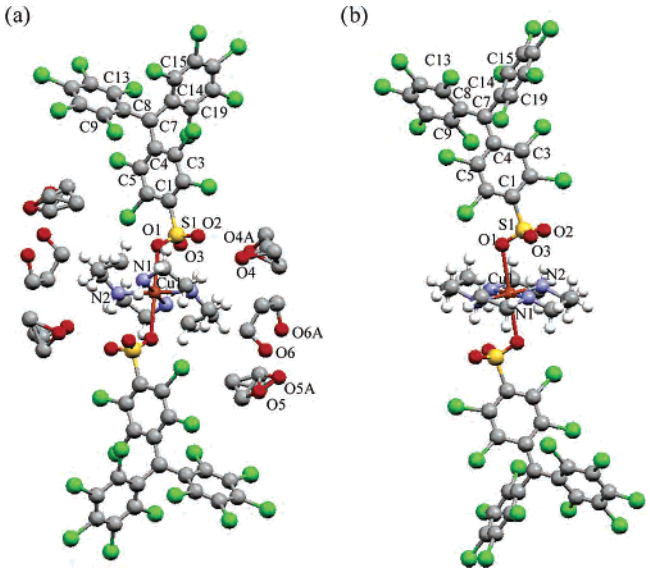

Figure 5. Structure of (a) $[Cu(cyclam)](PTMSO_3)_2 \cdot 6EtOH$ (**5a**) and (b) $[Cu(cyclam)](PTMSO_3)_2$ (**5b**). Only representative atoms are labeled.

Compound **5a** crystallizes as red plate-shaped crystals in the triclinic system, space group $P\bar{1}$ (Table 1). The asymmetric unit contains one molecule of $PTMSO_3^-$, half molecule of cyclam, and three EtOH molecules of crystallization (the latter shows a 1:1 disorder) in general positions (Figure 5a). Finally, the copper atom is located on a symmetric center. The structure of **5a**, with a stoichiometry of two $PTMSO_3^-$ molecules per copper ion, reveals a η^1-monodentate coordination of the sulfonate group with the copper cation through one O atom. The copper center shows an axially elongated octahedral geometry with four N atoms (cyclam ligand) placed in the equatorial plane and two O atoms from the $PTMSO_3^-$ radical anions in axial positions (Table S1, see Supporting Information).

The 3D crystal packing is determined by two major supramolecular interactions. First, multiple Cl···Cl contacts between $PTMSO_3^-$ anions of different complex molecules exist along the *ab* plane. The structure is further stabilized by a H-bond network, extended along the *ab* plane, between ethanol molecules placed in the voids left by the rectangular organization built up through Cl···Cl contacts from different complex molecules. The H-bonding network propagates along the *b* axis because of the interaction of ethanol molecules with the ligand molecule and also with the noncoordinating O atoms of the sulfonate groups (Figure 6). All of this together leads to a 2D alternated organic/inorganic layered structure, in which the monodentate coordination of the sulfonate groups to the copper center is responsible for the connection of the organic and inorganic layers.

[Cu(cyclam)](PTMSO$_3$)$_2$ (5b). Compound **5b** is obtained after the evacuation of all the ethanol molecules of crystallization from the as-synthesized compound **5a**. This is achieved simply by removal of the crystals from the mother liquor and exposure to the air. The structure of **5b** was obtained from the same crystal of **5a** after a crystal-to-crystal

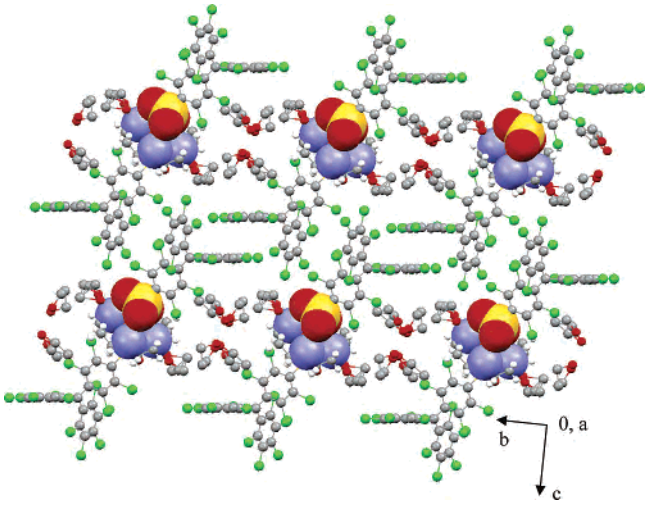

Figure 6. Crystal packing of [Cu(cyclam)](PTMSO$_3$)$_2$·6EtOH (**5a**) (copper coordination environment depicted in the space-filling mode).

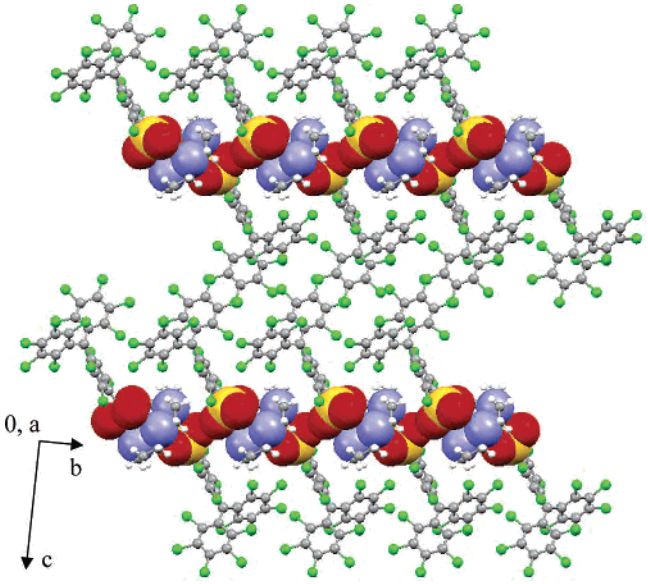

Figure 7. Crystal packing of [Cu(cyclam)](PTMSO$_3$)$_2$ (**5b**) (copper coordination environment depicted in the space-filling mode).

transformation[10,21] because of the evacuation of ethanol molecules of crystallization. Compound **5b** crystallizes in the triclinic system, space group $P\bar{1}$ (Table 1). The asymmetric unit is very similar to that of **5a** and contains one $PTMSO_3^-$ anion and one-half of a cyclam molecule in general positions, and the copper atom is in a symmetry center. The η^1-coordination mode of the sulfonate group is almost identical to the one described for **5a** (Figure 5b and Table S1, see Supporting Information).

The crystal packing is dominated by Cl···Cl contacts between the $PTMSO_3^-$ radicals, Cl···H−C contacts between anion moieties and the aliphatic backbone of cyclam, and π···H−C interactions between the aromatic rings of the anion and the aliphatic backbone of the ligand. Overall, this compound can be described as a 2D alternating organic/inorganic layered structure, with the layers extending along the *ab* plane (Figure 7). The major difference with respect to **5a** comes from the reorganization of the complex molecules because of the instability of the structure of **5a** after removal of the ethanol molecules. Basically, the Cl···Cl interactions of **5a** are not sufficient to support the voids left by the solvent. Thus, the reorganization results in the more compact structure of **5b**, visualized with a 25% reduction of the cell volume (Table 1). The sulfonate group in **5b** only plays the role of an axial monodentate ligand and does not participate in any other intermolecular interaction.

Structural Comparison. All studied compounds show a 2D alternated organic/inorganic layered structure. The organic layer is built up by the interaction of the chlorinated organic part of the $PTMSO_3^-$ molecules, whereas the inorganic layer is formed by the metal complex (with the exception of the pure organic compound **2**, where the inorganic layer is substituted by charge-assisted H-bonded disordered H_2O molecules). The main difference between compounds **3**, **4**, and **5** is the ability of the sulfonate group to be coordinated to the metal center. Despite having a nonreliable structure for **3**, the complete chemical and spectroscopic characterization ensures the presence of Na atoms that are coordinated to the $-RSO_3^-$ group, possibly together with H_2O molecules. On the contrary, no direct coordination of the sulfonate group to the Cu^{II} dication is found in **4**. The poor coordinating ability of the sulfonate group is well-known, but several groups have faced the challenge of controlling the coordination possibilities of the sulfonate group, and several examples, ranging from direct coordination to the metal to solvent-separated ion pair compounds, are well described. Shimizu and co-workers have determined that sulfonate ions do not efficiently displace solvent from the primary coordination sphere of most metal ions under hydrous conditions, except in the case of alkaline, larger alkaline earth ions, and silver(I) ions.[13] For the latter metals, a very rich variability on the coordination modes is described. Also Kennedy and co-workers have shown a clear trend of the degree of coordination and connectivity of the sulfonate group to the s-block metals as a function of the electronegativity of the metal, in a family of sulfonated azo dyes.[22] Thus, structures without direct sulfonate−metal coordination (type I) are found when the s-block metal ion has a Pauli electronegativity higher than 1.29. On the other hand, structures with simple $-RSO_3-M$ bonds (type II) are found with s-block metals with electronegativities in the range of 1.2−0.88. Finally, structures showing high connectivity between the $-RSO_3^-$ group and the metal ion (type III) are found when the Pauli electronegativities are below 0.88. The sodium compound **3** described in this work should be a type III structure since Na has a Pauli electronegativity

(21) (a) Uemura, K.; Kitagawa, S.; Fukui, K.; Saito, K. J. *J. Am. Chem. Soc.* **2004**, *126*, 3817−3828. (b) Kumar Maji, T.; Uemura, K.; Chang, H.-C.; Matsuda, R.; Kitagawa, S. *Angew. Chem., Int. Ed.* **2004**, *43*, 3269−3272. (c) Uemura, K.; Kitagawa, S.; Kondo, M.; Fukui, K.; Kitaura, R.; Chang, H.-C.; Mizutani, T. *Chem.−Eur. J.* **2002**, *8*, 3587−3600. (d) Biradha, K.; Fujita, M. *Angew. Chem., Int. Ed.* **2002**, *41*, 3392−3395. (e) Biradha, K.; Hongo, Y.; Fujita, M. *Angew. Chem., Int. Ed.* **2002**, *41*, 3395−3398. (f) Suh, M. P.; Ko, J. W.; Choi, H. J. *J. Am. Chem. Soc.* **2002**, *124*, 10976−10977.

(22) Kennedy, A. R.; Kirkhouse, J. B. A.; McCarney, K. M.; Puissegur, O.; Smith, W. E.; Staunton, E.; Teat, S. J.; Cherryman, J. C.; James, R. *Chem.−Eur. J.* **2004**, *10*, 4606−4615.

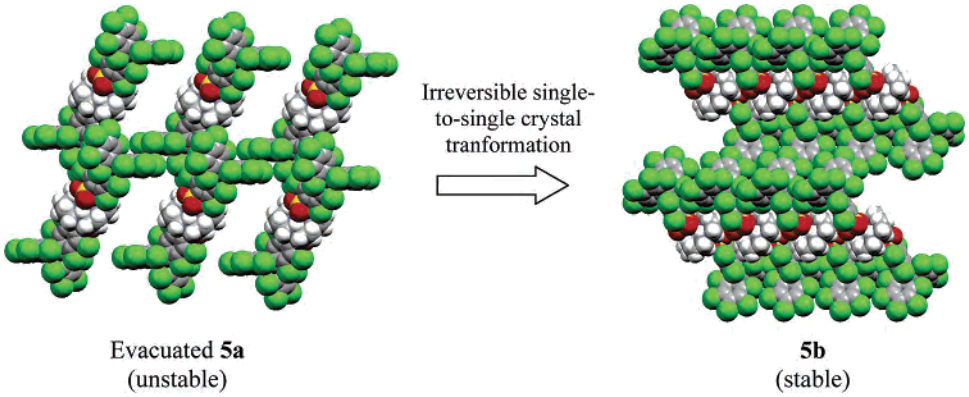

Figure 8. Single-to-single crystal rearrangement after evacuation of EtOH molecules from **5a** leading to **5b**.

value of 0.869. However, the high connectivity of Na to the $-RSO_3^-$ group could not be demonstrated because of the low quality of crystals, and the presence of water molecules cannot be discarded.[23] On the other hand, structure **4** is an example of a type I solvent-separated ion pair, also in line with both an electronegativity value for Cu of 1.9 and the well-known poor coordination capability of the sulfonate group toward transition metals.

However, very recent publications have shown that the sulfonate group is capable of coordinating dicationic copper if the ligands that complete the coordination of the metal have suitably placed C−H bonds that can stabilize the SO_3−M bond as an axial coordination.[24] To test this possibility with the $PTMSO_3^-$ radical anion, we chose the square-planar $[Cu(cyclam)]^{2+}$ cation with the aim that the cyclam backbone will stabilize the axial coordination of the sulfonate groups by H-bonding. The structural description of compounds **5a** and **5b** is the successful result of the strategy applied. The direct coordination of the sulfonate group to the copper center in a η^1-monodentate fashion in **5a** and **5b** is achieved because of the stabilization through H-bonding of the noncoordinating O atoms and the C−H and N−H residues of the ligand backbone.[25] Thus, the sulfonate group can now compete and displace the H_2O molecules from the coordination environment of the copper center, in contrast to **4**.

Thermal Stability Studies. Thermal stabilities of the crystal structure of compounds **2**, **3**, and **4** were determined by thermal gravimetric studies combined with infrared spectra and X-ray powder diffraction (XRPD). Thermal analysis of **2** and **3** shows no noticeable weight loss below 200 and 230 °C, respectively (Figure S2, see Supporting Information), beyond which decomposition occurs as confirmed by infrared spectra. On the other hand, thermogravimetric analysis of a crystalline sample of **4** indicates three weight losses (Figure S3, see Supporting Information). The first endothermic weight loss of 1.5% that can be assigned to the removal of one solvent ethanol molecule (theoretical value 2.3%) was observed between 70 and 95 °C. A second consecutive and gradual weight loss of 4.2% was then observed from 95 to 200 °C, which is attributed to the departure of the remaining ethanol molecule and two H_2O solvent molecules (theoretical value 4.1%). Finally, an abrupt weight loss attributed to decomposition was observed at 250 °C. Such a decomposition process was confirmed by infrared spectra.

In a separate experiment, a crystalline sample of **4** was heated in argon to 200 °C and then was studied by infrared spectra and XRPD. The infrared spectra confirms the total evacuation of the crystallization solvent molecules from the hydrogen-bonded network of **4**, and simultaneously, XRPD studies confirmed that **4** remains crystalline and stable up to 200 °C. Indeed, the XRPD pattern of the desolvated sample shows that the positions and intensities of all lines remain unchanged when compared with the theoretical XRPD pattern obtained from the crystal structure (Figure S4, see Supporting Information). This lets a potential accessible void volume of 11%, which represents a volume of 207.4 Å^3 compared to the 1882.1 Å^3 of the total cell volume.[26] The structural stability of desolvated **4** is remarkable because it is a structure maintained by a second-sphere coordination "soft" network.[27] We believe that the stability of **4** is directly related to the H-bond network described above and especially to the simultaneous six-member rings between two sulfonates of different layers through the copper-coordinated H_2O molecules. Also the multiple Cl···Cl contacts between the PTM derivatives within the organic layer stabilize the structure up to 200 °C.

Thermogravimetric studies were also performed with compound **5b**, showing no weight loss below 275 °C, at which point the decomposition starts. As detailed above, compound **5a** undergoes a rapid transformation to **5b** after the removal of the ethanol molecules of crystallization, which occurs at room temperature within a few seconds (Figure 8). The calculation of the void volume left by the evacuation

(23) Kennedy and co-workers also reported a few exceptions to their classification (see ref 22), for example, an unexpected solvent-separated ion pair in a sulfonate−sodium compound.

(24) (a) Cai, J.; Chen, C.-H.; Liao, C.-Z.; Yao, J.-H.; Hu, X.-P.; Chen, X.-M. *J. Chem. Soc., Dalton Trans.* **2001**, 1137−1142. (b) Mahmoudkhani, A. H.; Coté, A. P.; Shimizu, G. K. H. *Chem. Commun*. **2004**, 2678−2679.

(25) For H-bonding in organic sulfonates, see: Haynes, D. A.; Chrisholm, J. A.; Jones, W.; Motherwell, W. D. S. *CrystEngComm* **2004**, *6* (95), 584−588.

(26) Speak, A. L. *PLATON*; Utrecht University: Utrecht, The Netherlands, 1998.

(27) Dalrymple, S. A.; Shimizu, G. K. H. *Supramol. Chem.* **2003**, *15* (7−8), 591−606.

of the ethanol molecules in **5a** (a void volume of 31%)[26] suggests that the channels are too large and the structure is not stable. Thus, a rearrangement toward the more compact structure of **5b** is favored, as confirmed by the XRPD pattern of a microcrystalline sample of **5b** that agrees with the calculated pattern from its crystal structure.

Magnetic Properties. EPR measurements on $PTMSO_3H$ (**2**) and $PTMSO_3Na$ (**3**) compounds in solution showed one single line at $g = 2.0020$ ($\Delta H_{pp} = 4$ G) and 2.0023 ($\Delta H_{pp} = 1$ G), respectively, with no signal at half field, denoting that the organic radicals do not have noticeable interactions. On the other hand, the EPR measurements on solid polycrystalline samples of the Cu-containing compounds **4** and **5b** at room temperature showed a typical axial symmetry signal for an elongated octahedral Cu^{II} center at room temperature with $g_1 = 2.0060$($\Delta H_{pp} = 35$ G) and $g_2 = 2.265$ for **4** and $g_1 = 2.0199$ ($\Delta H_{pp} = 11.4$ G) and $g_2 = 2.0670$ for **5b**, with minor changes on the spectra at 120 K. The signal of the organic radical (typically with $g = 2.0030$) lies eclipsed under the intense signal of the copper in **4** and **5b**.

The magnetic properties of polycrystalline samples of **2**, **3**, **4**, and **5b** were measured on a SQUID magneto/susceptometer in the temperature range of 1.8−300 K at a constant magnetic field of 0.5 T. The temperature dependence of the product of the molar susceptibility and temperature (χT) for compounds **2**, **3**, and **4** can be found in the Supporting Information (Figures S5−S10). Compounds **2** and **3** exhibit a typical paramagnetic behavior in the 10−300 K temperature range, with χT product values that fully agree with the theoretical value of 0.375 emu K^{-1} mol^{-1} and expected for uncorrelated $S = 1/2$ moieties. Similarly, the χT product value for **4** also remains constant at 1.13 emu K mol^{-1}, which is in agreement with the theoretical value of 1.125 emu K^{-1} mol^{-1} expected for three uncorrelated $S = 1/2$ moieties (two $PTMSO_3^-$ radicals and one Cu^{II} ion). Below 10 K, the χT product slightly decreases in accordance with the presence of very weak intermolecular antiferromagnetic interactions. All magnetic behaviors were fitted to the Curie−Weiss law between 1.8 and 300 K, with $C = 0.37$, 0.37, and 1.12 emu K mol^{-1} and a Weiss constant of $\theta = -0.7$, -0.1, and -0.3 K for compounds **2**, **3**, and **4**, respectively.

Identical measurements performed in compound **5b** show the presence of stronger antiferromagnetic interactions resulting from the direct coordination of $PTMSO_3$ moieties to Cu^{II} ions (Figure 9). A χT value of 1.17 emu K mol^{-1} was obtained at 300 K, which is close to the theoretical 1.15 emu K mol^{-1} value expected for three isolated $S = 1/2$ spins and with a g factor of 2.04, as previously measured by EPR. When the temperature is lowered, $\chi_M T$ remains constant until 100 K, from which point it follows a continuous fall down to 0.78 emu K mol^{-1} at 1.9 K. The resulting experimental data was quantitatively analyzed on the basis of a linear three-spin model, using the following effective Hamiltonian, $H = -2J(S_{R1}S_M + S_MS_{R2})$, modified to take into account the presence of intermolecular interactions (θ) in the molecular-field approximation.[28] The resulting parameters for the best fit were $2J/k_B = -4.6$ K and $\theta = -0.1$ K, fixing $g = 2.04$. From the comparison with the antiferromagnetic coupling constants found for similar systems using the monocarboxylated PTM radical ($2J/K_B = -30$ to -50 K),[9a] it can be deduced that the carboxylate group is a better moiety than the sulfonate moiety in terms of magnetic communication between the radical and the metal ion. The qualitative analysis of the torsion angles of the sulfonate-containing ring in **5b** with respect to the corresponding monocarboxylated PTM radical Cu complex[9a] does not reveal a clear difference that could induce a high variation in the spin density over the ligand groups responsible for this result. Theoretical studies are needed to understand this point. Nevertheless, it cannot be excluded that a η^2-coordination mode of the sulfonate group with respect to the metal may enhance the magnetic interaction.

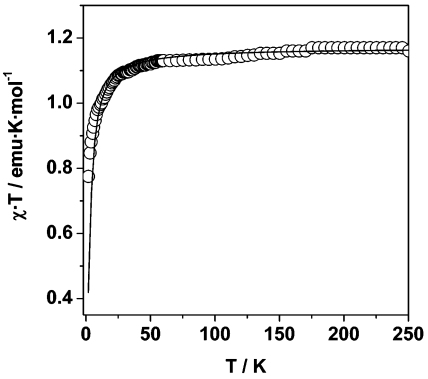

Figure 9. Temperature dependence of the product of the magnetic susceptibility and the temperature for complex **5b**. The solid line was calculated for a linear three-spin model as described in the manuscript.

Summary

In summary, we have reported the synthesis of a novel pure organic radical of the PTM family bearing one sulfonic group, compound $PTMSO_3H{\cdot}3H_2O{\cdot}0.5$hexane (**2**). We have explored for the first time the coordination capabilities of a radical bearing a sulfonate group: one example with a nonparamagnetic alkaline metal, compound $PTMSO_3Na{\cdot}H_2O$ (**3**), and one example with a paramagnetic transition metal ion such as Cu^{II}, compound $[Cu(py)_2(H_2O)_4](PTMSO_3)_2{\cdot}2H_2O{\cdot}2$EtOH (**4**). In the latter compound, we have shown that a solvent-separated ion pair (SSIP) situation in the structure precludes magnetic communication between the two distinct magnetic centers. We have also demonstrated that is possible to overcome this situation and force the direct coordination of the sulfonate group to the copper center by choosing a metal complex bearing a ligand suitable to stabilize the axial coordination of the sulfonate moiety, as occurs in compound $[Cu(cyclam)](PTMSO_3)_2{\cdot}6$EtOH (**5a**). This compound readily losses the solvent molecules of crystallization upon exposure to open air and rearranges to compound $[Cu(cyclam)](PTMSO_3)_2$ (**5b**) in a single-to-single-crystal transformation. The direct coordination of the organic radical through the sulfonate group is reflected on an enhanced antiferromagnetic coupling between the para-

(28) Ishimaru, Y.; Kitano, M.; Kumada, H.; Koga, N.; Iwamura, H. *Inorg. Chem.* **1998**, *37*, 2273−2280.

magnetic centers. We believe that this study represents an overview of the crystal engineering possibilities of the novel sulfonate derivative PTM organic radical, in line with other studies on the sulfonate group coordination, but focusing on the introduction of magnetic functionality within the metal−organic approach that yielded remarkable layered hybrid organic−inorganic structures. We have been successful in the use of the radical $PTMSO_3^-$ anion as building block in metal−organic coordination compounds and have shown that the antiferromagnetic coupling between the organic and Cu^{II} open-shell species is significantly lower than that for the monocarboxylated PTM derivatives. Theoretical studies will be undertaken to compare the differences in spin density between the carboxylate and sulfonate groups. Further experimentation aimed at exploration of the additional coordination abilities of the PTM-SO_3^- radical, such as different coordination modes or its reactivity with other metal ions, and the design of new molecular multifunctional magnetic materials via incorporation of more $-SO_3^-$ moieties in the PTM skeleton, is currently underway.

Acknowledgment. This work was supported by DGI, Spain (Project MAT2003-04699) and DGR Catalonia (Project 2005SGR00362). D.M. is grateful to the Generalitat de Catalunya for a postdoctoral grant. X.R. acknowledges a Juan de la Cierva contract from MEC Spain.

Supporting Information Available: X-ray crystallographic files in CIF format for structures **2**, **4**, **5a**, and **5b**, table of selected bond distances and angles for all compounds (Table S1), and complemetary structural (Figure S1), thermogravimetric (Figure S2 and S3), XRPD studies (Figure S4), and magnetic measurements for compounds **2**, **3**, and **4** (Figure S5−S10). This material is available free of charge via the Internet at http://pubs.acs.org.

IC060182J